

Oxygen Diffusion and Permeability in Alkylaminothionylphosphazene Films Intended for Phosphorescence Barometry Applications

Christine N. Jayarajah, Ahmad Yekta, Ian Manners, and Mitchell A. Winnik*

Department of Chemistry, University of Toronto, 80 St. George St., Toronto, Ontario, Canada M5S 3H6

Received December 28, 1999; Revised Manuscript Received May 1, 2000

ABSTRACT: This paper describes the application of a technique based on luminescence quenching to measure the diffusivity and permeability of molecular oxygen in a series of poly(*n*-alkylaminothionylphosphazenes) (C_n PTP) and in un-cross-linked high molecular weight PDMS. The glass transition temperatures (T_g) of these polymers decrease from 4 °C for $n = 2$ to –18 °C for $n = 6$. Experiments performed on thin films of these highly permeable polymers show that oxygen diffusivity is sensitive to the microstructure of these polymers and that the diffusion coefficient for oxygen increases as T_g decreases. In contrast, the oxygen solubility in these polymers is not very sensitive to the nature of the alkyl substituent. Both the oxygen diffusion coefficient D_{O_2} and the oxygen solubility S_{O_2} are smaller for this series of polymers than for PDMS.

Introduction

Over the past decade, a number of new sensor technologies have been developed that depend on luminescence measurements to detect and quantify the amount of oxygen in a gas or a fluid.¹ These technologies are designed around the concept of a fluorescent or phosphorescent dye dissolved or dispersed in polymer matrix, typically a thin film. Oxygen is a powerful quencher of the excited states of a broad spectrum of dyes. As oxygen partitions into or out of the sensor layer, the extent of quenching changes and is detected by a change in luminescence intensity or luminescence decay rate of the dye in the matrix. We are particularly interested in the use of these polymer films to measure air-pressure profiles across the surface of an object exposed to a flow of wind. This technique, called “phosphorescence barometry” by Gouterman,² is now used as a method for measuring and visualizing air-pressure profiles across the model of an airplane or a turbine blade subjected to different air velocities in a wind tunnel.^{3,4} The engineers who coat these objects with a solution of the polymer and dye in a solvent refer to the coating as “pressure-sensitive paint” (PSP).⁵

The underlying principle of this method is very simple. If a film of polymer on a substrate is exposed to air, the solubility of oxygen in the film will be proportional to the partial pressure of oxygen (p_{O_2}). If the film is thin and the air pressure is different at different points on the surface, the local concentration of O_2 will depend on the local air pressure at that point on the surface. A dye dissolved in the film will sense that local concentration of O_2 when excited by light. A digital video image of the illuminated object subjected to a wind flow will have brighter luminescence in regions of lower surface air pressure.^{3–5}

Many of the problems and limitations of the technique are associated with the choice of dye and the choice of polymer. The materials aspects of sensor technology prompt us to revisit a traditional issue in polymer science: understanding the factors that affect the diffusivity and permeability of oxygen in polymers.⁶ Sensor applications normally require polymers with a high permeability to oxygen. Many oxygen sensors are based upon commercially available, curable silicone rubber

formulations. The limited evidence available about these polymers is that oxygen permeability is very sensitive to the detailed chemical structure of the silicone polymer, which, for commercial resins, is not always revealed by the supplier and varies with the extent of cure.⁷ One of our contributions to this field has been the synthesis of a new linear polymer, poly(*N*-butylaminothiolphosphazene) (C_4 PTP),⁸ with a glass transition well below room temperature but above that of poly(dimethylsiloxane) (PDMS). This polymer gives good performance in PSP applications without the need for cross-linking.⁹ To improve upon this material, we need to prepare new derivatives and to determine how they interact with oxygen.

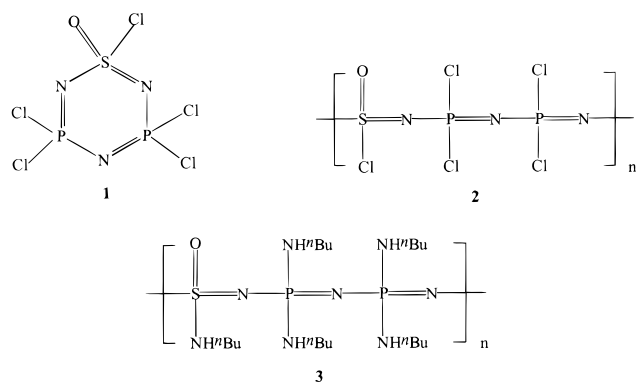
Gas diffusion and permeation in polymers is normally measured by a transport experiment involving a thin polymer membrane as first described by Barrer.¹⁰ In a typical experiment, one exposes the membrane to a certain partial pressure of gas at $t = 0$ and monitors the flux of gas through a film of known thickness. At steady state, the flux of gas is constant. One determines the permeability P of the gas from the steady-state flux per unit area and the diffusion coefficient of the gas from the lag time associated with the approach to steady state. The permeability (P) and the diffusion coefficient (D) are related to the solubility (S) per unit external pressure of the gas by the expression

$$P = DS$$

Thus, bulk-averaged D and P values can be obtained from classical diffusivity measurements, and the gas solubility S can be calculated from the expression $S = P/D$.

Here we are concerned with how the structure of a series of poly(*n*-alkylaminothiolphosphazene) (C_n PTP) polymers affects oxygen diffusion and solubility in their films. These polymers have glass transition temperatures near or below room temperature. As a consequence, one cannot fabricate free-standing films for traditional membrane diffusion measurements. Under these circumstances, spectroscopic methods based upon fluorescence or phosphorescence quenching offer a special advantage for the study of oxygen diffusion in polymers. The polymer film can be supported on a solid

Scheme 1



substrate, and the area of measurement is small, typically a few square millimeters. This can simplify the problem of obtaining a film of uniform thickness across the entire area of measurement. One prepares a film with a luminescent dye dissolved in the polymer. When the film is illuminated at a wavelength at which the dye absorbs light, the dye becomes electronically excited and then fluoresces or phosphoresces at a longer wavelength. Oxygen is a powerful quencher of this emission, and dyes with long-lived excited states are particularly sensitive to oxygen quenching.¹¹ The decrease in emission intensity as O_2 diffuses into the film or the growth in intensity as O_2 diffuses out of the film provides the information from which D_{O_2} and P_{O_2} are calculated.¹²

Experimental Section

Materials. Samples of poly[*n*-alkyl(amino)thionylphosphazenes] were synthesized by Pang and Park in the Manners' group by the following route.^{8,12} A sample of cyclic pentachlorothionylphosphazene (Scheme 1) (2 g, 6.1 mmol) was polymerized in a sealed Pyrex tube at 200 °C for 1 h to give a 70% yield of polymer 2. An *N*-alkylamine was gradually added with a syringe to a stirred solution of polymer 2 (0.7 g, 2.1 mmol) in 50 mL of CH_2Cl_2 at 0 °C, and the reaction was allowed to proceed for 12 h at room temperature. The solution was then concentrated under vacuum to one-seventh of its initial volume and added dropwise into water. The polymer was purified by repeated steps of dissolution–reprecipitation, using water (three times) and then a mixture of methanol and water (1:1, v/v; three times) as the precipitant. In this way they obtained polymeric product 3. (In Scheme 1, a butyl side chain is shown in polymer 3 as an example of the alkyl group.) After drying the sample in vacuo, the yield of the light yellow elastomer thus obtained was typically 90%.

Gel permeation chromatography (GPC) measurements were carried out with a Waters 2690 Separations Module chromatograph operating at 35 °C with three American Polymer Standards cross-linked polystyrene/divinylbenzene columns (pore sizes 10^5 , 10^4 , and 500 Å) and tetrahydrofuran (THF, spectrograde from Aldrich) as the eluent. The detector was a Waters 410 differential refractometer operating at 32 °C. Samples were dissolved in a solution of 0.1% tetrabutylammonium bromide in THF. The molar masses reported in Table 1 are nominal, based upon polystyrene standards. The glass transitions temperatures for the polymers (T_g) were measured with a Perkin-Elmer DSC-7 differential scanning calorimeter equipped with a TAC 7/Unix instrument controller.

The absolute molecular weight for C_6PTP , as a representative example, was determined by static light scattering experiments using a goniometer from Brookhaven Instruments Corporation equipped with a He–Ne laser operating at a wavelength of 632.8 nm. The BI-200SM goniometer consists of a rigid rotating arm upon which the main detector optics are fixed and is controlled by a stepping motor that enables the automatic selection of the desired scattering angle. Measurements for seven different concentrations of the polymer

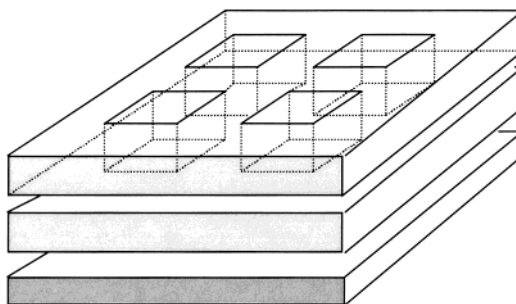


Figure 1. Four troughs are cut into the top piece of Teflon, which is placed on a second piece of Teflon. Both of the Teflon pieces are placed on top of a stainless steel support and tightly screwed together. The glass supports are placed into the troughs, and the polymer solution containing the dye is pipetted on top of the glass supports.

solution in THF were made at seven angles ranging from 30° to 150°. Each solution was filtered twice through a Gelman Science arcodisk filter with a 0.2 mm pore size before injection into the sample cell, which is contained within a quartz vat filled with toluene. A Chromatix KMX-16 differential refractometer operating at a wavelength of 632.8 nm and calibrated with NaCl solutions was used to determine the value of the refractive index increment ($dn/dc = 0.0806 \text{ mL/g}$) of the polymer solutions. The data fit a Zimm plot and yielded a value of $M_w = (1.43 \pm 0.40) \times 10^5 \text{ g/mol}$. The second virial coefficient $A_2 = (1.47 \pm 0.15) \times 10^{-4} \text{ mol mL}^{-1} \text{ g}^{-2}$. The radius of gyration R_G ($20 \pm 2 \text{ nm}$) was determined from a plot of Kd/R_θ versus $\sin^2(\theta/2)$.

High molecular weight PDMS ($M_w = 500\,000$, $2.5 \times 10^6 \text{ cSt}$, $T_g = -127 \text{ °C}$ ¹³) was purchased from Polysciences, Inc., Warrington, PA. Platinum octaethylporphyrine (PtOEP, from Porphyrin Products, Inc.) was used as the probe dye in all of the polymers under consideration.

Sample Preparation. Two Teflon molds, with a series of troughs cut into them, were used to prepare the film samples. The molds were assembled from a 1.0 cm thick plate into which a series of holes ($13 \times 13 \text{ mm}$) were cut. This sheet was placed on top of a second Teflon plate with identical length and width, which was first placed between two highly polished stainless steel sheets in a Carver press at 300 psi and heated at 270 °C for an hour in order to give it a smooth finish. The two Teflon layers were set on a stainless steel support, and then the three pieces were tightly screwed together, as shown in Figure 1. The smaller mold contained four troughs and the larger 24 troughs.

Polymer solutions (about 20 wt %) were prepared in THF into which the dye PtOEP was dissolved. Substrate-supported films were prepared by pipetting a few milliliters of polymer–dye solution onto square Pyrex substrates ($13 \times 13 \times 1 \text{ mm}$), which had been placed inside each of the troughs in the mold. Polymer films without the dye were also prepared in this way for control experiments to ensure that there was no interfering background emission. The mold was then placed into a large evaporating dish and partially covered with a large watch glass to allow slow evaporation of the solvent. To improve film quality, the solvent was constrained to evaporate slowly over 3 days in the dark and at room temperature 23 °C, after which the films were placed in a vacuum for 1–2 days.

Measuring the thickness of low- T_g polymer films is not easy. Prior to performing each time-scan experiment, the thickness of each film was measured with a micrometer as follows. A piece of PET (poly(ethylene terephthalate)) film was placed on top of the film and subjected to a light but uniformly distributed pressure. Following this, the combined thickness of the PET sheet-plus-film-plus-substrate was measured. The film thickness was then calculated by subtracting the thicknesses of the glass substrate and PET film from the combined thickness. Relatively thick films ranging from about 70 to 400 μm were prepared. Thick films make the thickness measurement more reliable and increase the time span of the diffusion process to allow sufficient data to be acquired in time-scan

Table 1. GPC and Glass Transition Data for the PTP Polymers

polymers	M_w^a	M_n^a	polydispersity	T_g (°C)
C ₁ PTP ^c	5.0×10^3	3.3×10^3	1.5	22
C ₂ PTP	1.8×10^3	9.7×10^4	1.8	4
C ₃ PTP	2.2×10^5	1.0×10^5	2.1	6
C ₄ PTP	1.2×10^5	5.9×10^4	2.1	-16
C ₆ PTP ^b	2.7×10^5	1.6×10^5	1.6	-18
C ₇ PTP	2.3×10^5	1.4×10^5	1.7	

^a Nominal molecular weights based upon polystyrene standards.

^b By light scattering, $M_w = (1.4 \pm 0.4) \times 10^5$. ^c The molecular weight is dramatically underestimated by GPC (see ref 21).

experiments. The PET sheet was peeled off of each film after the thickness measurement. For PDMS, a piece of Teflon was used instead of PET since PDMS adheres strongly to PET.

Photophysical Experiments. A Perkin-Elmer UV/vis Lambda 6 spectrometer was used to obtain the absorbance spectra for dye solutions and film samples, and a SPEX Fluorolog 2 spectrometer equipped with a DMA 3000 data system was used to obtain emission spectra.

To perform time-scan fluorescence experiments, the film on the glass substrate was placed in a cuvette supported with a piece of Teflon, and the cuvette was sealed with a rubber septum. Two syringe needles were inserted through the rubber septum into the cuvette to allow either N₂ or air to flow in and out. One of these needles was left open to air, while the other was used to connect the cuvette to either a compressed nitrogen or air cylinder during the course of the time-scan experiments. The plastic cuvette containing the sample was placed in the sample chamber of the emission spectrometer. Initially, the sample in the cuvette was allowed to equilibrate in approximately 1 atm of nitrogen. Following this, the needle connected to the nitrogen cylinder was switched to air at 1 atm. This changeover took a few seconds. The measurement of luminescence intensity for each experiment began with this rapid change in flowing gas, from nitrogen to air, and vice versa. The emission intensity was detected at right angles. All experiments were performed at room temperature (23 ± 1 °C).

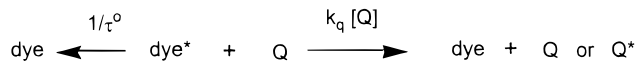
The luminescence decay time of the dye in the polymer films in the absence of oxygen quencher was obtained as follows. The Pyrex-substrate-supported film was placed in a copper sample holder and placed in a vacuum chamber in the optical path of the beam of a frequency-doubled (532 nm) Nd:YAG laser (Spectra Physics DCR 3). After the vacuum chamber was flushed with N₂ several times, the sample was allowed to equilibrate in 1 atm of pure N₂. Following sample irradiation with short pulses (ca. 6 ns) of light, the phosphorescence emission was detected using a 650 nm broad band-pass filter and a fast-gated Hammamatsu 956 photomultiplier connected to a Tektronix model 7912AD transient digitizer.

Results and Discussion

Materials. The polymers we examine were prepared by the method shown in Scheme 1. A sample of cyclic pentachlorothionylphosphazene (**1**) was polymerized in a sealed Pyrex tube at 200 °C for 1 h to give polymer **2** in approximately 70% yield. Polymer **2** serves as the precursor to the polymers of interest: Aliquots of this polymer in CH₂Cl₂ at 0 °C were treated with various *N*-alkylamines (C_{*n*}H_{2*n*+1}NH₂, with *n* = 1–7) to form the series of poly(*n*-alkylaminothionylphosphazenes) (C_{*n*}PTP) that we describe below. As shown in Table 1, as the alkyl substituent was increased in length, the glass transition temperature of the polymer decreased.

Films containing approximately 10⁻⁴ M PtOEP were prepared on Pyrex substrates. The luminescence of these films was examined as a function of time following rapid change of the surrounding atmosphere from nitrogen to air and from air to nitrogen. These results are described and interpreted below, following a presentation of the theory used to interpret the results.

Theory. The kinetic scheme for a typical dynamic luminescence quenching reaction is shown in Scheme

Scheme 2

2. A dye is excited either with a pulse of light or by steady-state illumination. In competition with its luminescence (either fluorescence or phosphorescence), the excited dye (dye*) can encounter a second species Q, the quencher. From this simple mechanism, one derives the Stern–Volmer (SV) equation (eq 1), which serves as the point of departure for all discussions of fluorescence and phosphorescence quenching involving mobile species in polymers. In this expression, Φ refers to the luminescence quantum yield, I is the luminescence intensity, and τ is the lifetime of the dye. The superscript 0 refers to the absence of quencher. The term k_q represents the phenomenological bimolecular rate constant for quenching, and $[Q]$ is the molar concentration of quencher.

$$\frac{\Phi^0}{\Phi} = \frac{I^0}{I} = \frac{\tau^0}{\tau} = 1 + k_q\tau^0[Q] \quad (1)$$

Quenching for Systems at Equilibrium. Oxygen is a powerful quencher of dye luminescence. In applying the SV expression to oxygen quenching in polymers, one assumes that when the oxygen concentration in the film has been allowed to come to equilibrium, the quencher concentration is macroscopically uniform throughout the sample and that oxygen is at its equilibrium solubility limit ($[O_2]_{eq} = [Q]_{eq} \equiv Q_{eq}$). The luminescence intensity of the polymer film is measured in the absence of oxygen (I^0) and upon reaching equilibrium (I_{eq}) with an external atmosphere containing a certain partial pressure of oxygen, p_{O_2} . This expression predicts that I^0/I_{eq} and τ^0/τ_{eq} increase linearly with increasing external partial pressure of oxygen.

According to Henry's law, at low to moderate pressures, the equilibrium solubility of oxygen Q_{eq} is proportional to p_{O_2} . Thus, the Henry's law constant of gas solubility, S , can be incorporated into eq 1 through the relation $Q_{eq} = S_{O_2}p_{O_2}$.

Oxygen is a very effective quencher of both excited singlet and triplet excited states. In fluid solution, k_q approaches diffusion control ($k_q \approx k_{diff}$).¹⁴ From the theory of partially diffusion-controlled reactions,¹⁵ one derives eq 2 for the steady-state value of k_{diff} .

$$k_q = k_{diff} = (4\pi N_A/1000)DR_{eff} \quad (2)$$

In this expression N_A is Avogadro's number, and D is the sum of the diffusion coefficients of the interacting species. In polymer films, oxygen diffusion is much faster than the diffusion of the dye, and one sets $D = D_{O_2}$. Thus, one obtains

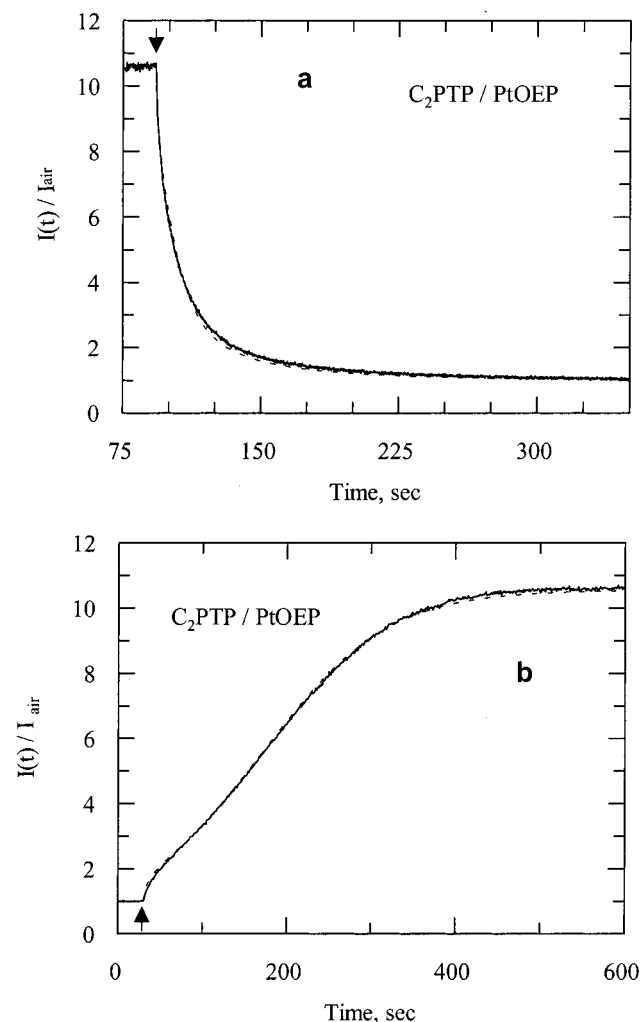
$$\frac{\tau^0}{\tau_{eq}} = \frac{I^0}{I_{eq}} = 1 + \left(\frac{4\pi N_A \tau^0 R_{eff}}{1000} \right) (D_{O_2} S_{O_2}) p_{O_2} \quad (3)$$

Note that, in terms of eq 3 for $k_q \approx k_{diff}$, if the product $D_{O_2}[Q]$ is small, one needs a dye with a long τ^0 in order to observe significant quenching.

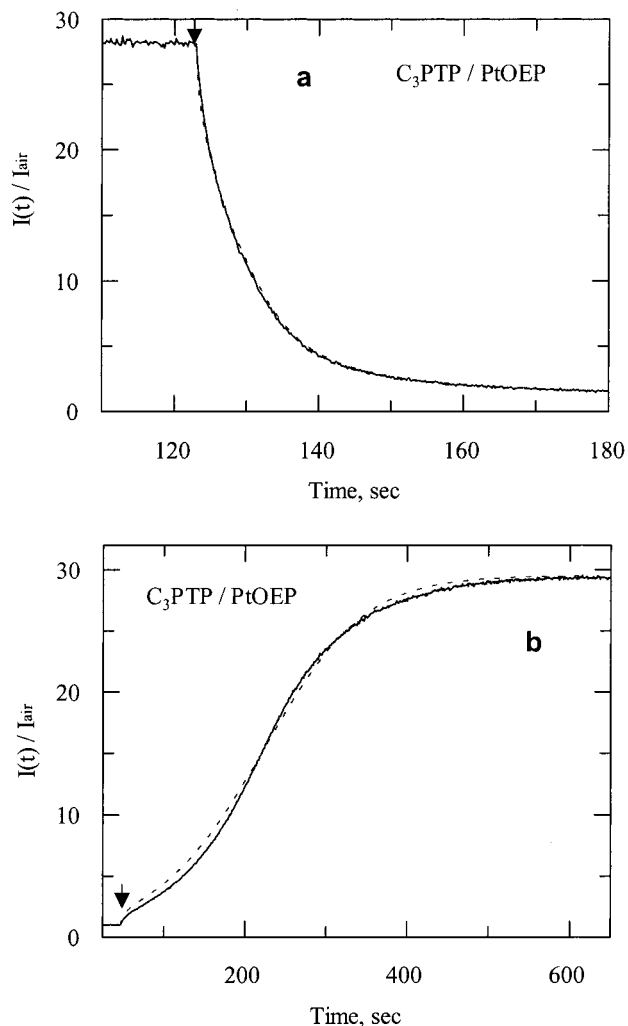
In eqs 2 and 3, R_{eff} is an effective interaction distance at which quenching takes place and is smaller than the true interaction distance R . By defining R_{eff} in this way, one sidesteps the controversy of the role of spin statistics in the quenching of singlet and triplet states by oxygen.^{16,17} There is a subtle feature of eq 3 that is difficult

Table 2. Lifetimes (τ^0) of PtOEP in the Absence of Oxygen and the Effective Diffusion Length L_{eff} of Oxygen in Each Polymer

polymer	τ^0 (μs)	L_{eff} , nm	polymer	τ^0 (μs)	L_{eff} , nm
C ₂ PTP	105	180	C ₇ PTP	96	590
C ₄ PTP	103	500	PDMS	61	850
C ₆ PTP	98	600			

**Figure 2.** Time scan of the phosphorescence of 81 ppm PtOEP in a 93 μm thick film of C₂PTP. In this and all subsequent time scan experiments, the films are supported on Pyrex plates. The emission is observed at 645 nm during steady-state excitation at 537 nm. The continuous traces represent the experimental data; the dashed lines show the theoretical fits to eq 12. In this and all subsequent time scan experiments, the time scale on the x -axis begins arbitrarily at a given time, whereas the actual onset of the experiment is indicated by a vertical arrow on the plot. (a) Sorption experiment: the sample is initially equilibrated in an atmosphere of pure N₂ ($p_{\text{O}_2} = 0.0$ atm), and the chamber is at once flushed with air ($p_{\text{O}_2} = 0.02$ atm); fitting parameters $L^2/D = 180$, $B = 9.7$. (b) The sample is initially equilibrated with air, and the chamber is at once flushed with pure N₂; fitting parameters $L^2/D = 173$, $B = 9.6$.

to treat. The theory of partially diffusion-controlled reactions predicts that R_{eff} varies with D , with $1/R_{\text{eff}}$ approaching $1/R$ as D approaches zero.^{18,19} It would be very useful to have independent data for R_{eff} and D to test this idea for O₂ quenching in polymers. Without this information, we follow the path of others and assume that R_{eff} is a constant in our system. In analyzing our data, we set $R_{\text{eff}} = 1.0$ nm.

**Figure 3.** Phosphorescence time scan experiments for 499 ppm PtOEP in a 128 μm thick film of C₃PTP. (a) Sorption experiment; fitting parameters $L^2/D = 160$, $B = 27.1$. (b) Desorption experiment; fitting parameters $L^2/D = 142$, $B = 28.5$.

Sorption and Desorption Experiments. When a polymer film containing a luminescent dye is suddenly exposed to an atmosphere that is rich or poor in oxygen, oxygen will diffuse into or out of the film until a new equilibrium is established. Time scan experiments under steady illumination will detect the decay or growth in emission intensity. From analysis of these data, the D_{O_2} values can in principle be determined. The challenge in interpreting this type of experiment properly has been the development of a theory connecting the SV equation to the concentration profiles generated by gas diffusion. We follow the approach of Yekta et al.,^{20a} who used numerical methods both to simulate and to analyze real experimental data. An earlier derivation of eqs 5a and 5b was reported by Mills.^{20b}

Gas diffusion follows Fick's second law,

$$\frac{\partial c(x,t)}{\partial t} = D \frac{\partial^2 c(x,t)}{\partial x^2} \quad (4)$$

where $c(x,t)$ is the concentration of the dissolved gas at time t and distance x within the film and D its diffusion coefficient. One assumes a Henry's law dependence of the gas concentration in the polymer and introduces boundary conditions appropriate for oxygen diffusion from the atmosphere into a film (an oxygen sorption

experiment) or oxygen diffusion from the film into the atmosphere (an oxygen desorption experiment). For the former case, the concentration of quencher oxygen absorbed by the film can be related to the exposure time by eq 5a.

oxygen sorption: $Q(x, t) = Q_{\text{eq}} \left[1 - \frac{4}{\pi} \sum_{n=\text{odd}} \frac{1}{n} \exp\left(-\frac{n^2 \pi^2 D t}{4L^2}\right) \sin\left(\frac{n\pi x}{2L}\right) \right]$ (5a)

For the latter case, the concentration of quencher oxygen remaining in the film is given by

oxygen desorption: $Q(x, t) = Q_{\text{eq}} \left[\frac{4}{\pi} \sum_{n=\text{odd}} \frac{1}{n} \exp\left(-\frac{n^2 \pi^2 D t}{4L^2}\right) \sin\left(\frac{n\pi x}{2L}\right) \right]$ (5b)

These equations pertain to a film of thickness L , mounted on a substrate with only one side exposed to the oxygen.

When the concentration of oxygen in the film changes, the emission intensity, $I(t)$, changes with time. The measured intensity is the sum of the incremental intensities of the dye molecules located at various depths in the film, which in turn are related to the concentration profile of oxygen in the film, $Q(x, t)$. From the SV equation, we obtain the expression

$$\frac{\partial I^0}{\partial I(x, t)} = I + \frac{B}{Q_{\text{eq}}} Q(x, t); \quad \partial I^0 = I^0 dx/L \quad (6)$$

and defining $\rho(x, t) = Q(x, t)/Q_{\text{eq}}$ leads to

$$I(t) = \frac{I^0}{L} \int_0^L \frac{dx}{1 + B\rho(x, t)} \quad (7)$$

where B is constant and is defined as the ratio of the emission intensities for the film at equilibrium in the presence and absence of oxygen.

$$B = \frac{I^0}{I} - 1 = (4\pi N_A/1000)\tau^0 R_{\text{eff}}(D_{\text{O}_2} S_{\text{O}_2}) p_{\text{O}_2} = K p_{\text{O}_2} \quad (8a)$$

$$K = (4\pi N_A/1000)\tau^0 R_{\text{eff}}(D_{\text{O}_2} S_{\text{O}_2}) \quad (8b)$$

Time-Scan Oxygen Sorption and Desorption Experiments. To study oxygen sorption and desorption kinetics, one changes the external atmosphere surrounding a polymer film containing a luminescent dye and monitors the intensity of emission from the film as a function of time. This type of measurement is often called a time-scan experiment. To interpret the data with eq 7 in terms of O_2 diffusion in the polymer, one must first determine the value of B , which is calculated from the initial and final equilibrium intensities employing eq 8. The integral in eq 7 can be evaluated numerically to obtain the best value of D_{O_2}/L^2 as a fitting parameter. Hence, the bulk diffusion coefficient D_{O_2} can be calculated without knowledge of either k_q or τ^0 . From the magnitude of D_{O_2} , one can calculate the mean diffusion distance L_{eff} of an oxygen molecule during the lifetime of the excited state from the expression $L_{\text{eff}} = (6D\tau^0)^{1/2}$.

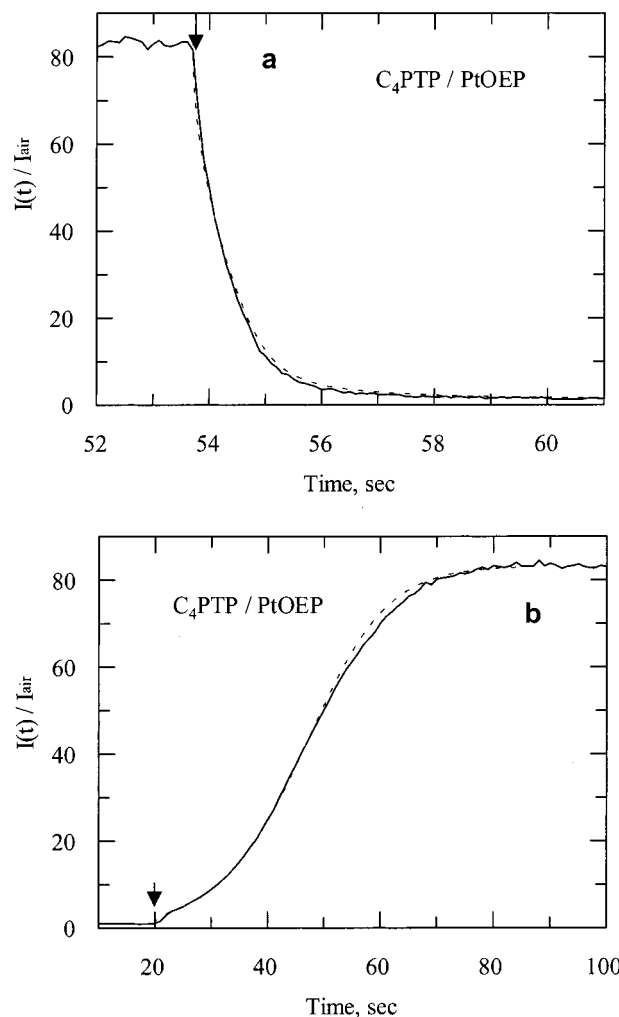


Figure 4. Phosphorescence time-scan experiments for 256 ppm PtOEP in a 85 μm thick film of C_4PTP . (a) Sorption experiment; fitting parameters $L^2/D = 20$, $B = 82.7$. (b) Desorption experiment; fitting parameters $L^2/D = 16.9$, $B = 82.3$.

Equation 7 indicates that the rate of intensity decay depends on Q_{eq} , which has been neglected in older reports of similar experiments. Furthermore, it predicts that the rate of emission intensity decay when O_2 diffuses into a polymer film will be much faster than the rate of emission intensity growth when O_2 diffuses out of the same film, even when the molecular diffusivity remains unchanged.²⁰ This difference between oxygen sorption and desorption experiments is clearly manifested in the time-scan data presented in Figures 2–6.

Evaluating P_{O_2} from B requires an independent measurement of τ^0 and knowledge of R_{eff} , which we assume to have a value of 1.0 nm. The lifetimes, τ^0 , of PtOEP at room temperature in each of the different polymers in a pure nitrogen environment were obtained from pulsed laser experiments. Values are presented in Table 2.

C_1PTP . C_1PTP is a very brittle polymer that is difficult to work with. We were able to prepare films containing PtOEP. However, no change in emission intensity was observed when air at 1 atm was flushed into a cell containing a film of C_1PTP in a nitrogen environment or when nitrogen was flushed into a cell containing the film in air at 1 atm. Since the B value is very small, no meaningful data on oxygen diffusion are

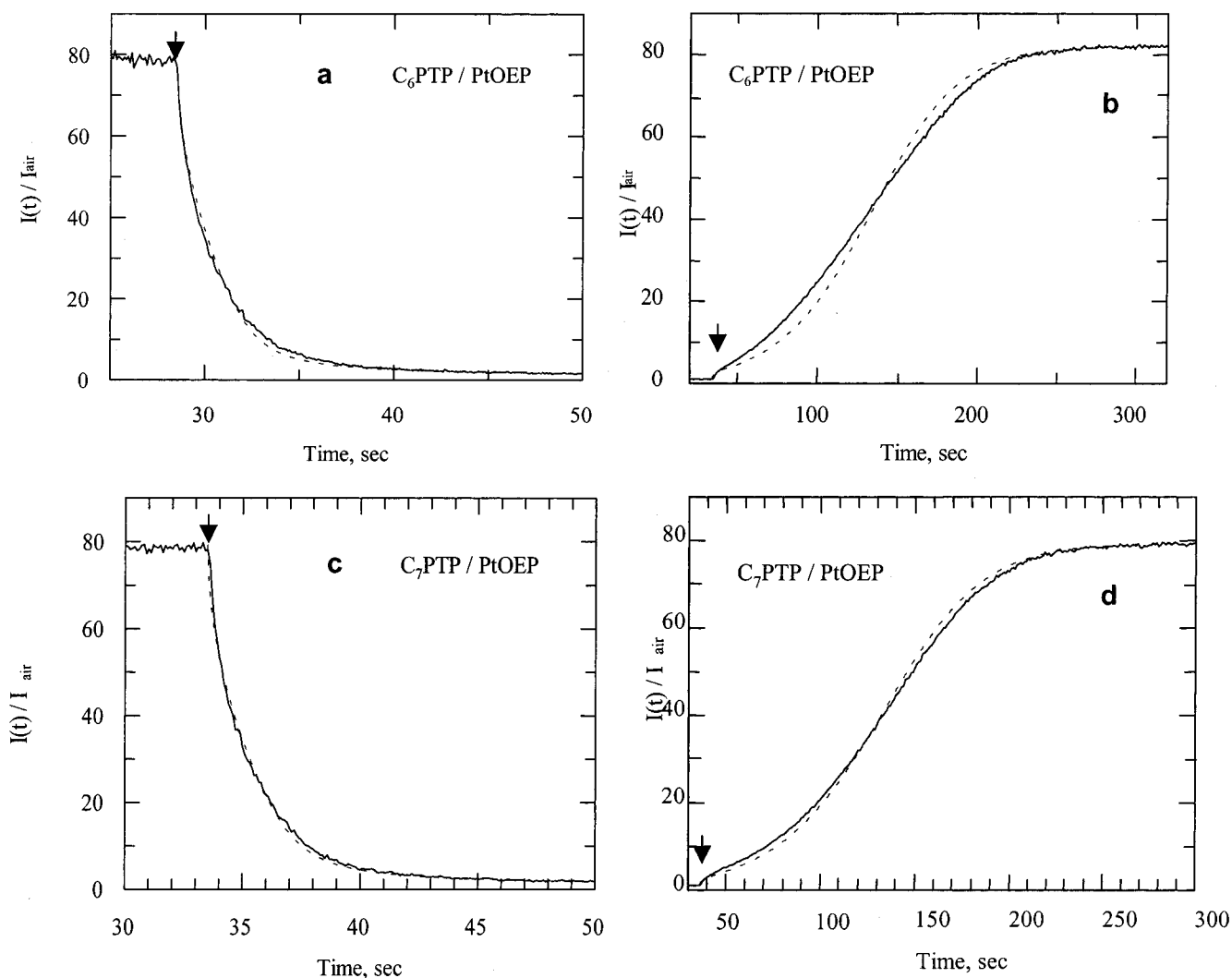


Figure 5. Phosphorescence time scan experiments: (a) and (b) for 89.7 ppm PtOEP in a 210 μm thick film of C_6PTP supported on Pyrex glass. (a) Sorption experiment; fitting parameters $L^2/D = 61.1$, $B = 79.8$. (b) Desorption experiment; fitting parameters $L^2/D = 60.7$, $B = 80.9$. (c) and (d) for 146 ppm PtOEP in a 185 μm thick film of C_7PTP supported on Pyrex glass. (c) Sorption experiment; fitting parameters $L^2/D = 55.0$, $B = 78.2$. (d) Desorption experiment; fitting parameters $L^2/D = 59.4$, $B = 78.5$.

accessible by this method. We assume that the low B value is due to small oxygen permeability in this polymer.

C_2PTP . Shown in Figure 2 are two time-scan experiments performed on the same $\text{C}_2\text{PTP}/\text{PtOEP}$ film with a thickness (L) of 93 μm . In the oxygen sorption experiment shown in Figure 2a, the decrease in relative intensity occurs over a period of 106 s when air at 1 atm is flushed into a cell containing the film in a nitrogen environment. In Figure 2b, we see the response when oxygen is rapidly flushed out of the cell with a stream of nitrogen. As the oxygen diffuses out of the film, the increase in intensity is more gradual and takes place over about 470 s. This interesting feature of the experiment is predicted by the theory as expressed in eqs 8 and 10. When the data are fitted to numerically eq 8 by means of a least-squares method, we obtain an optimum estimate of the ratio D_{O_2}/L^2 . In actual practice, we estimate a value of D_{O_2}/L^2 from the midpoint of each curve. This value is then used to simulate a theoretical intensity profile. Values of D_{O_2}/L^2 are then varied until a best fit is obtained. As shown in Figure 3, the theoretical curves match reasonably well with the experimental data. For the C_2PTP film, analysis of the sorption experiment yielded values of $B = 9.7$, L^2/D_{O_2}

$= 180$ s, and $D_{\text{O}_2} = 4.8 \times 10^{-7}$ cm^2/s . From the desorption experiment we find $B = 9.6$, $L^2/D_{\text{O}_2} = 173$ s, and $D_{\text{O}_2} = 5.0 \times 10^{-7}$ cm^2/s . Average values calculated from 10 experiments carried out with two film samples of different thicknesses are $D_{\text{O}_2} = (5.0 \pm 0.4) \times 10^{-7}$ cm^2/s and $B = 9.7 \pm 0.2$. Using the average value of B , the permeability P_{O_2} was calculated to be $(6.2 \pm 0.1) \times 10^{-13}$ $\text{mol cm}^{-1} \text{s}^{-1} \text{atm}^{-1}$. From the P_{O_2} and the average D_{O_2} , the oxygen solubility was calculated to be $S_{\text{O}_2} = (1.2 \pm 0.1) \times 10^{-3}$ M atm^{-1} .

C_3PTP . The sorption scan performed on a C_3PTP film with a thickness of 128 μm is shown in Figure 3a, where the intensity decreases and approaches equilibrium in 60 s. Analysis of this scan yields $B = 27.1$, $L^2/D_{\text{O}_2} = 160$ s, and $D_{\text{O}_2} = 1.02 \times 10^{-6}$ cm^2/s . Figure 3b presents the corresponding desorption experiment in the intensity increases over 450 s to its new equilibrium value in a pure N_2 atmosphere and gives $B = 28.5$, $L^2/D_{\text{O}_2} = 142$ s, and $D_{\text{O}_2} = 1.15 \times 10^{-6}$ cm^2/s . On the basis of eight experiments on two film samples of different L , the average $D_{\text{O}_2} = (1.2 \pm 0.2) \times 10^{-6}$ cm^2/s and the average $B = 28.4 \pm 1.0$ for C_3PTP . From the average values for D and B , the average P_{O_2} is calculated to be $(1.8 \pm 0.1) \times 10^{-12}$ $\text{mol cm}^{-1} \text{s}^{-1} \text{atm}^{-1}$ and $S_{\text{O}_2} = (1.5 \pm 0.3) \times 10^{-3}$ M atm^{-1} .

Table 3. Averaged Values Calculated from Time Scan Experiments

polymer	T_g (°C)	B	$D_{O_2}^a$	$P_{O_2}^b$	$S_{O_2}^c$
C ₂ PTP	4	9.7 ± 0.2	0.50 ± 0.04	0.62 ± 0.01	1.2 ± 0.1
C ₃ PTP	6	28 ± 1	1.2 ± 0.2	1.8 ± 0.1	1.5 ± 0.3
C ₄ PTP	-16	74 ± 6	4.0 ± 0.6	4.8 ± 0.4	1.2 ± 0.2
C ₆ PTP	-18	80 ± 1	6.2 ± 0.8	5.4 ± 0.1	0.87 ± 0.11
C ₇ PTP		74 ± 4	6.0 ± 0.5	5.1 ± 0.3	0.85 ± 0.08
PDMS	-127	170 ± 59	20 ± 4	18 ± 6	0.91 ± 0.37

^a D values are 10^{-6} cm² s⁻¹. ^b P values are 10^{-12} mol cm⁻¹ s⁻¹ atm⁻¹. ^c S values are 10^{-3} M atm⁻¹.

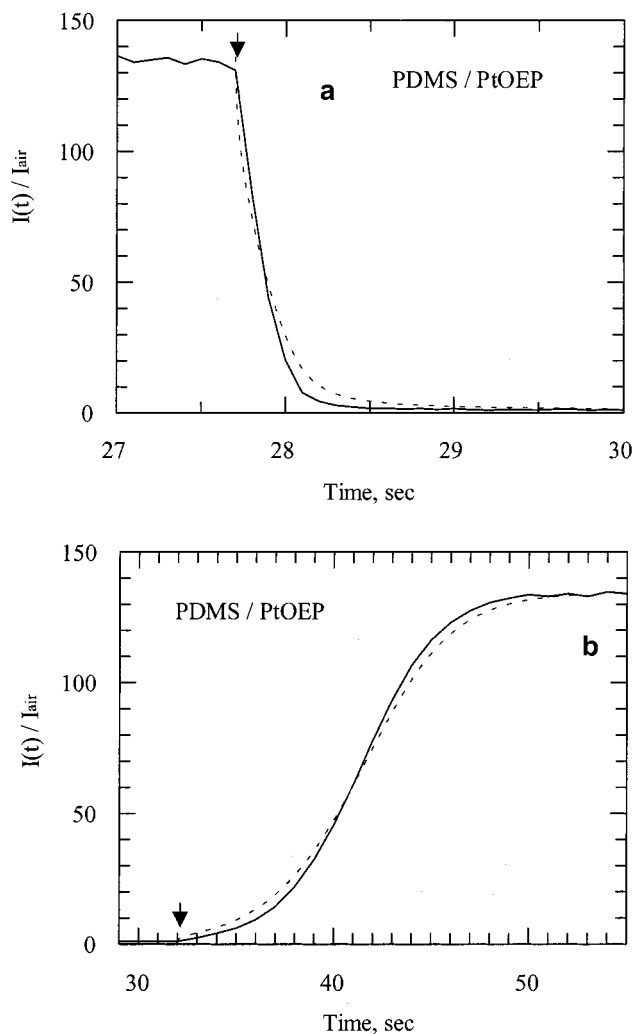


Figure 6. Phosphorescence time scan experiments for 495 ppm PtOEP in a 99 μ m thick film of PDMS supported on Pyrex glass. The emission is observed at 644 nm during steady-state excitation at 536 nm ($p_{O_2} = 0.02$ atm). (a) Sorption experiment; fitting parameters $L^2/D = 5.55$, $B = 135$. (b) Desorption experiment; fitting parameters $L^2/D = 5.17$, $B = 133$.

C₄PTP. A sorption scan performed on a C₄PTP/PtOEP film with $L = 85$ μ m is shown in Figure 4a, where the decrease in intensity occurs in about 6.3 s. The calculated $L^2/D_{O_2} = 20$ s, $B = 82.7$, and $D_{O_2} = 3.61 \times 10^{-6}$ cm²/s. In Figure 4b we present the corresponding desorption time-scan intensity data, which take about 60 s to reach equilibrium. Analysis of this scan gives $B = 82.3$, $L^2/D_{O_2} = 16.9$ s and $D_{O_2} = 4.28 \times 10^{-6}$ cm²/s. The average values calculated from 20 experiments on five film samples of varying L are $D_{O_2} = (4.0 \pm 0.6) \times 10^{-6}$ cm²/s and $B = 74.0 \pm 5.9$. From these average values for D_{O_2} and B , the average P_{O_2} is $(4.8 \pm 0.4) \times 10^{-12}$ mol cm⁻¹

s⁻¹ atm⁻¹ and the average S_{O_2} is $(1.2 \pm 0.2) \times 10^{-3}$ M atm⁻¹.

C₆PTP and C₇PTP. Time-scan experiments for C₆PTP and C₇PTP are similar in form to those shown in Figures 2–4. A representative sorption and desorption trace for each polymer and the corresponding best fit to the data are presented in Figure 5. Mean experimental values of B and calculated values of D_{O_2} , P_{O_2} , and S_{O_2} are presented in Table 3.

PDMS. Sorption and desorption time-scan experiments for a high molecular weight sample of PDMS are presented in Figure 6. The noteworthy features of these experiments are, first, that the B values are large, particularly in comparison with the values for the various C_{*n*}PTP polymers, and second, that relaxation rates are fast. Compared to the C_{*n*}PTP described above, we also find greater variability in the B values ($B = 170 \pm 59$). The D_{O_2} value is significantly larger than those for the C_{*n*}PTP polymers but is of the same magnitude as that reported earlier for oxygen diffusion in cross-linked PDMS matrices. For instance, Cox et al.²¹ report 3.55×10^{-5} cm² s⁻¹ for D_{O_2} in pure PDMS at 25 °C. When the D_{O_2} and B values are combined, we find an oxygen solubility very similar to that for the other polymers described above.

Interpreting the Data. All of the polymers for which quenching data could be obtained exhibited response profiles to exposure to air that decayed at a much faster rate than the recovery profiles obtained when oxygen was flushed out of the cell. This type of behavior would not occur if oxygen concentration in the film were uniform, but this situation is explicitly predicted by eq 7 for the change of boundary conditions appropriate for sorption and desorption experiments. The precision of L^2/D_{O_2} values, obtained from repeated experiments on an individual film, are excellent, with a typical standard error of 5%. Values of D_{O_2} calculated from multiple film samples are less precise. The largest source of error in these experiments is the determination of the film thickness. Values of P_{O_2} are calculated directly from the measured value of B . These values do not depend on the thickness of the film, but they do depend on the value assumed for R_{eff} .

The lack of signal for C₁PTP is an indication that the permeability of oxygen is too low for quenching to be observed with PtOEP as the probe. It may be possible to obtain meaningful data for this polymer by using a dye with a longer lifetime or by using pure oxygen at higher pressures instead of air as the surrounding atmosphere. Alternatively, one might be able to carry out measurements for C₁PTP at higher temperatures and then extrapolating values to room temperature.

The value for D_{O_2} in C₄PTP obtained here ($D_{O_2} = (4.0 \pm 0.6) \times 10^{-6}$ cm²/s) is significantly smaller than that reported previously ($D_{O_2} = (1.4 \pm 0.4) \times 10^{-5}$ cm² s⁻¹). This surprised us, and as a consequence, we repeated this experiment many times. When we looked carefully at the sample preparation method used previously, we noted that the films were dried in air for 3 days but had not been placed in a vacuum afterward. Attempts to duplicate this preparation method gave D_{O_2} values closer to the published value. This result suggests that residual solvent may have acted as a plasticizer to increase the diffusivity of oxygen in the polymer.

We recently had the need, as part of a study of C₄-PTP block copolymers,²¹ to repeat these experiments on a newly synthesized sample of C₄PTP. The new results

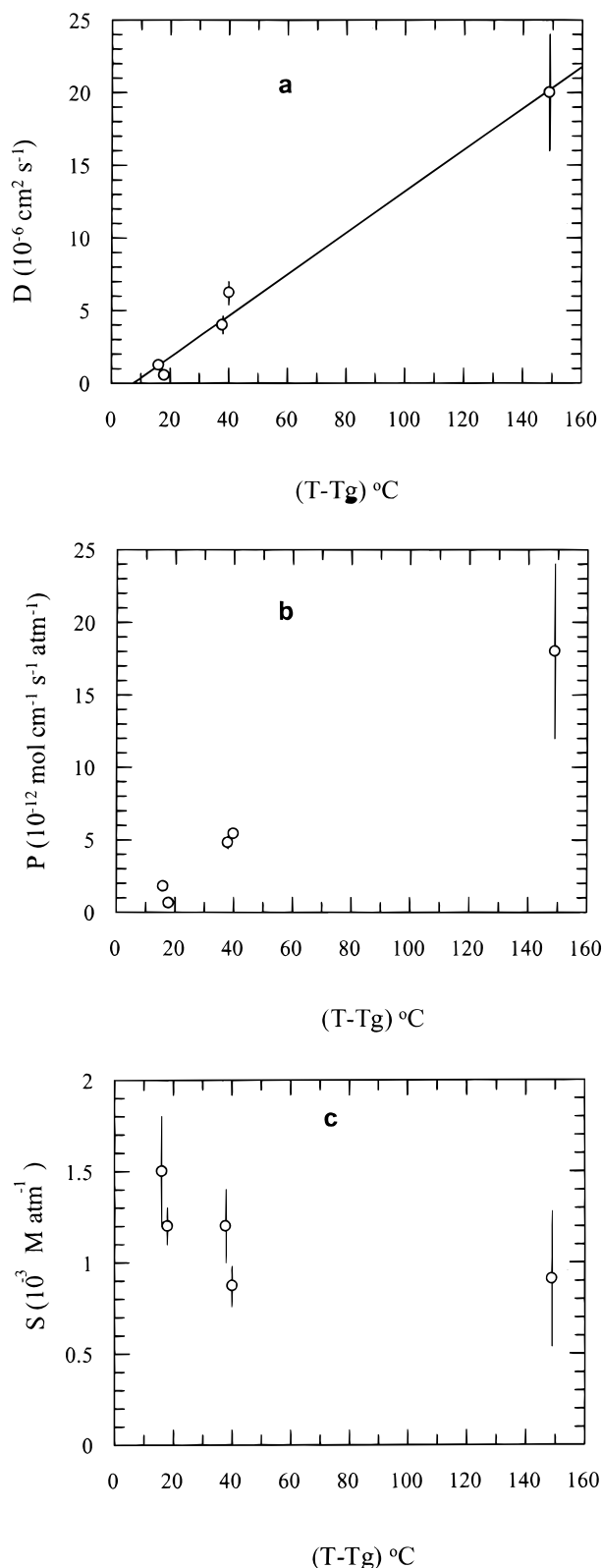


Figure 7. Plots of D_{O_2} , P_{O_2} , and S_{O_2} vs $(T - T_g) ^\circ\text{C}$, where T is room temperature ($22 ^\circ\text{C}$) and T_g is the glass transition temperature of the different polymers. The large error bar for D_{O_2} in PDMS is related in large part to the difficulty in measuring the film thickness for this polymer.

for D_{O_2} and P_{O_2} are essentially identical to those reported here.

In the series of polymers $C_n\text{PTP}$ with $n = 2-7$, the major consequence of the change in pendant group is a decrease in T_g with increasing alkyl chain length. We

find that while S_{O_2} values are not very sensitive to the changes in polymer structure, values of D_{O_2} and P_{O_2} increase with decreasing T_g . We plot these values vs $(T - T_g)$ for D_{O_2} in Figure 7a, for P_{O_2} in Figure 7b, and for S_{O_2} in Figure 7c. For the $C_n\text{PTP}$ series of polymers, the largest change in D_{O_2} occurs between $n = 2$ and $n = 3$; the polymers with $n = 4$ and 6 have similar values of T_g and similar values of D_{O_2} . By comparison with the $C_n\text{PTP}$ polymers, the permeability and diffusivity of oxygen in PDMS are significantly higher. Cox et al. suggested that the relatively large diffusivity in PDMS is due to the high flexibility of the $-\text{Si}-\text{O}-$ bond and weak intermolecular interaction²² in this polymer.

Summary

We have used phosphorescence quenching experiments to study the kinetics of sorption and desorption of oxygen from a series of poly(*N*-alkylaminothiophosphazene) ($C_n\text{PTP}$) polymers, with alkyl groups ranging from methyl to heptyl, as well as a linear high molecular weight sample of poly(dimethylsiloxane). The intensity-time profiles were fitted to a model that couples Fickian diffusion to Stern-Volmer quenching kinetics and takes rigorous account of the concentration profile of the diffusing gas molecules. For the $C_n\text{PTP}$ polymers we find D_{O_2} values ranging from 0.5×10^{-6} to $6 \times 10^{-6} \text{ cm}^2/\text{s}$, significantly smaller than that found for PDMS ($20 \times 10^{-6} \text{ cm}^2/\text{s}$). S_{O_2} values were comparable for the entire series polymers, including PDMS. When the D_{O_2} values for all of the polymers were plotted against $(T - T_g)$, a straight line was obtained.

Acknowledgment. We thank Peter Park for measuring T_g and M_w , M_n by GPC. Materials and Manufacturing Ontario (MMO) and NSERC Canada are acknowledged for their support of this research.

References and Notes

- (1) Demas, J. N.; DeGraff, B. A. *J. Chem. Educ.* **1997**, *74*, 690-695.
- (2) Kavandi, J.; Callis, J.; Gouterman, M.; Khali, G.; Wright, D.; Green, E. *Rev. Sci. Instrum.* **1990**, *61*, 3340-3347.
- (3) Moshasrov, V.; Radchenko, V.; Fonov, S. *Luminescent Pressure Sensors in Aerodynamic Experiments*; Central Aerohydrodynamic Institute (TsAGI): Moscow, 1998.
- (4) Gouterman, M. *J. Chem. Educ.* **1997**, *74*, 697-702.
- (5) Liu, T.; Campbell, B. T.; Burns, S. P.; Sullivan, J. P. *Appl. Mech. Rev.* **1997**, *50*, 227-246.
- (6) (a) Neogi, P., Ed.; *Diffusion in Polymers*; Marcel-Dekker: New York, 1996. (b) Crank, J., Park, C. S., Eds.; *Diffusion in Polymers*; Academic Press: New York, 1968.
- (7) Masoumi, Z.; Stoeva, V.; Yekta, A.; Winnik, M. A.; Manners, I. In *Polymers and Organic Solids*; Shi, L., Zhu, D., Eds.; Science Press: Beijing, 1997; pp 157-168.
- (8) Ni, Y.; Park, P.; Liang, M.; Massey, J.; Waddling, C.; Manners, I. *Macromolecules* **1996**, *29*, 3401-3408.
- (9) Pang, Z.; Gu, X.; Yekta, A.; Masoumi, Z.; Coll, J. B.; Winnik, M. A.; Manners, I. *Adv. Mater.* **1996**, *8* (9), 768.
- (10) Barrer, R. M. *Diffusion in and Through Solids*; Cambridge University Press: New York, 1951.
- (11) (a) Birks, J. B. *Photophysics of Aromatic Molecules*; Wiley-Interscience: New York, 1971. (b) Lakowicz, J. *Principles of Fluorescence Spectroscopy*; Plenum: New York, 1983.
- (12) Masoumi, Z.; Stoeva, V.; Yekta, A.; Pang, Z.; Manners, I.; Winnik, M. A. *Chem. Phys. Lett.* **1996**, *261*, 551-557.
- (13) Brandrup, J.; Immergut, E. H., Eds.; *Polymer Handbook*, 3rd ed.; John Wiley: New York, 1989.
- (14) Nemzek, T. L.; Ware, W. R. *J. Chem. Phys.* **1975**, *62*, 477-489.
- (15) Rice, S. A. In *Chemical Kinetics*; Bamford, C. H., Tipper, C. F. H., Compton, R. G., Eds.; Elsevier: New York, 1985; Vol. 25.

- (16) For reasons associated with spin statistics, the quenching of excited triplet states (dye^*3) by O_2 is often slower than the quenching of singlet excited states (dye^*1). For studies in solution see: (a) Gijzeman, O. L. J.; Kaufman, F.; Porter, G. *J. Chem. Soc., Faraday Trans. 2* **1973**, *69*, 708–720. (b) Patterson, L. K.; Porter, G.; Topp, M. R. *Chem. Phys. Lett.* **1970**, *7*, 612–614. See also: (c) Jones, P. F. *J. Polym. Sci., Part B: Polym. Lett.* **1968**, *6*, 487. (d) Nowakowska, P. F.; Najbar, J.; Waligora, B. *Eur. Polym.* **1976**, *12*, 387.
- (17) For a more recent discussion of spin statistics, particularly for oxygen quenching in polymer films, see: (a) Charlesworth, J. M.; Gan, T. H. *J. Phys. Chem.* **1996**, *100*, 14922–14927. (b) Guillet, J. E.; Andrews, M. *Macromolecules* **1992**, *25*, 2752–2756.
- (18) Martinho, J. M. G.; Winnik, M. A. *J. Phys. Chem.* **1987**, *91*, 3640–3644.
- (19) Pilling, M. J.; Rice, S. A. *J. Chem. Soc., Faraday Trans. 2* **1975**, *71*, 1563–1571.
- (20) (a) Yekta, A.; Masoumi, Z.; Winnik, M. A. *Can. J. Chem.* **1995**, *73*, 2021–2029. (b) Mills, A.; Chang, Q. *Analyst* **1992**, *117*, 1461–1466.
- (21) Ruffolo, R.; Evans, C.; Liu, X.-H.; Ni, Y.; Pang, Z.; Park, P.; McWilliams, A.; Gu, X.; Lu, X.; Yekta, A.; Winnik, M. A.; Manners, I. *Anal. Chem.* **2000**, *72*, 1894–1904.
- (22) (a) Cox, M. E.; Dunn, B. *J. Polym. Sci., Part A: Polym. Chem.* **1986**, *24*, 621. (b) Gao, Y.; Baca, A. M.; Wang, B.; Ogilby, P. R. *Macromolecules* **1994**, *27*, 7041.

MA992164+